# Investigation of self-heating and damage progression in woven carbon fibre composite materials, following the fibres direction, under static and cyclic loading

Laura Muller, Jean-Michel Roche, Antoine Hurmane, François-Henri Leroy, Catherine Peyrac, Laurent Gornet

# Investigation of self-heating and damage progression in woven carbon fibre composite materials, following the fibres direction, under static and cyclic loading

Laura Muller[a], Jean-Michel Roche[a], Antoine Hurmane[a], François-Henri Leroy[a], Catherine Peyrac[b], Laurent Gornet[c]

[a]DMAS, ONERA, Université Paris Saclay, F-92322 Châtillon - France
laura.muller@onera.fr
[b]CETIM, FCM, 52 avenue Félix Louat, 60300 Senlis, France
[c]Ecole Centrale de Nantes, GeM, UMR CNRS 6183, 1 rue de la Noë, 44321 Nantes, France

**Keywords:** experimental mechanics, thermoelasticity, self-heating, fatigue, thermoplastic composites

**Abstract**

Infrared thermography is commonly used as a non-destructive testing technique for damage monitoring of composite materials under mechanical loadings. Self-heating tests consist in monitoring the stabilized heating of a material submitted to cyclic loading for increasing values of stress level. It appears that the load threshold from which the thermal behaviour changes can be related to the fatigue limit of the tested material. In this paper, this stress threshold is compared to the heating of a woven thermoplastic composite material submitted to a monotonic tensile test. Indeed, during a quasi-static tensile test, the material temperature cools down, due to thermoelastic effect, before warming up again, due to both viscous effects and first damage evolutions. The comparison, which is made for the warp direction only, is also based on microscopic optical scanning of the specimen edge and passive acoustic monitoring. It is shown that thermal changes detected in the composite samples are associated with damage occurring under both static *and* cyclic loading, for similar stress levels. This result indicates that the static tests make it possible to estimate a damage threshold, therefore a potential fatigue limit, even faster than with self-heating tests, which opens very promising prospects as for the determination of the fatigue limit of woven composite materials reinforced by carbon fibre yarns.

## 1. Introduction

The mechanical characterization of a material often involves two major studies, which are the mechanical characterization under quasi-static loading and the study of fatigue performance.
The analysis in quasi-static regime consists in applying a monotonous load until failure on the specimen in order to characterize it mechanically. The mechanical behaviour (brittle or ductile) and its own characteristics such as its strain at ultimate failure, its maximum stress, its elasticity range described by its Young's modulus, etc. are thus obtained. This study enables to determine the performance of the material after manufacturing [9].
Fatigue implies that a part or a structure subjected to low-level but repeated loading will eventually break under cyclic stress. The characterization tests of this phenomenon consist in recording the number of cycles to failure N of a specimen associated with different load levels S, in order to set an S-N curve, called the Wöhler curve. In particular, at low stress levels, the S-N curve tends towards a horizontal asymptote, indicating that below a certain stress threshold, the material no longer breaks under the effect of fatigue, and is used to size critical structures that should not fail.
These two complementary domains are used to characterize the material in its nominal state and over its service life, and to design the structures consequently. The methodologies were initially developed for metallic materials and have been extended and adapted to the case of composite materials.

However, while quasi-static tests are easily and quickly achievable, the same cannot be said for fatigue tests. The latter require an experimental campaign of several months, carried out on a large number of samples, in order to finally approach an estimate of the fatigue limit. In addition, the fatigue behaviour differs according to the type of material, alloys (steel, aluminum or titanium), or composites (laminated or woven), making it sometimes difficult to detect and apply an endurance or fatigue limit. This is because metallic materials tend to remain undamaged for a very long time, until the first crack is initiated, which quickly causes the material failure. In contrast, composite materials show signs of small-scale damage from the first cyclic loading, but with a rather slow evolution, until an acceleration linked to the coalescence of cracks, which leads to failure [9].
Therefore, a new methodology based on the monitoring of thermal properties of the material has been developed over the last twenty years. The methodology consists in monitoring the heating of the material submitted to several steps of increasing load level, each step constituted of a limited number of blocks of fatigue cycles with increasing amplitudes. It has been validated for metals [1]–[3], [10], [11] and for thermoset and thermoplastic reinforced composite materials [5], [6], [12], [13] that the stress level associated with the change of thermal behaviour during self-heating tests is connected to the fatigue limit determined on the classic Wöhler curves. The major advantage of this equivalence lies in the reduction of the test duration and of the number of tested specimens.

In the present article, the relevance of self-heating tests for a fast fatigue limit estimation is assumed, i.e. it is assumed that the stress associated with the change of thermal behaviour during self-heating tests is an estimation of the fatigue limit determined from the Wöhler curves. It is also assumed that damage mechanisms (cracks, debonding, fibre breaks) are the same for both static and fatigue tests, and that between these two types of tests, only the kinetics of damage occurrence varies.
The aim of this study is then not to discuss the relevance of self-heating tests for fatigue limit estimation but to illustrate the similarities between thermal changes spotted for woven composite materials under quasi-static and cyclic loading. In both cases, the thermal analysis is completed with optical observations and acoustic monitoring.
The objective is twofold:

- Illustrate how the thermal monitoring of quasi-static tensile tests can also provide similar thermal and mechanical data on the fatigue behaviour of a woven composite material.
- Reinforce the thermal study with damage monitoring via acoustic and optical data, to prove that the change of thermal behaviour in both types of tests is indeed associated with the same damage phenomenon.

Two woven composite materials, reinforced with carbon fibres, are considered. Static and self-heating tests are carried out in the fibres direction of the material.

In section 2, the specifications of the materials of our study are provided (2.1), followed by the presentation of the application of thermographic monitoring during static and cyclic loading, leading to the justification of our approach (2.2). Then, the test protocols set up is detailed (2.4). Section 3 is dedicated to the thermal analysis of quasi-static (3.1) and self-heating tests (3.3), consolidated by acoustic emission and microscopic observations, for both tests (3.2 and 3.3). The results are then analyzed and discussed in Section 4, highlighting the advantages and limitations of our study.

## 2. Materials and procedures

### 2.1 Material and conditioning

The materials used in this study are of the woven composites which offer the advantage of being less sensitive to damage propagation compared to the unidirectional ones, despite slightly lower mechanical performance in the fibre direction. They are also more resistant to out-of-plane impacts, which makes them more and more attractive in the aeronautical field. However, monitoring and modelling their damage is more difficult to implement. Therefore, many works rely on non-destructive testing methods, such as thermal and acoustic monitoring, to display and model the damage mechanisms of woven composites under static or cyclic loading [22].
In this study, carbon fibres are chosen because of their high-performance applications. Two materials are considered: one with a thermoset matrix, a very common type of composite, and the other with a

thermoplastic matrix, which is gaining interest because of its ability to be recycled. The epoxy resin is widely used for aeronautical applications, while the PA66 matrix is already widely used for automotive application.

Thus, the first material is a 2 mm thick, 3-ply composite, constituted of 8-harness satin carbon fibres (G1151) reinforced with thermoset epoxy RTM6 matrix. Its pattern is represented in Figure 1, with the warp fibres appearing in grey and the weft fibres in white. The carbon/epoxy composite is very strong and light, and is widely used in the aeronautical field. It is manufactured under press at Onera from pre-impregnated fibres.
The second material is a 2 mm thick, 8-ply composite, constituted of a 2/2 balanced twill carbon fibres (T700) reinforced with thermoplastic polyamide matrix PA66, schematized in Figure 2. It is manufactured by TEPEX, using Bond Laminates, with a fibre volume of 45%. It is currently used in automotive and sport applications.

The PA66 resin has the particularity to be very sensitive to moisture absorption: the polyamide can absorb from 2% to 5% moisture, depending on the relative humidity [23], [24]. This important sensitivity to moisture has a direct impact on the mechanical properties [20], [25]. To guarantee the consistency of the experimental campaigns, the tested samples have to be conditioned with a controlled relative humidity (RH) rate. In this study, they are conditioned at ambient temperature, at $RH = 50\%$. The conditioning is ensured by desiccators, in which the conditioned air is generated by saturate salted solutions [26] and regularly controlled. The tests are carried out when the sample has reached a constant relative moisture level, which means that its mass is stabilized. Furthermore, the absorption and desorption kinetics of a composite material are so slow compared to the characteristic time of RH evolution that it can be assumed that the RH rate remains constant over the whole duration of the mechanical tests even if they are carried out in a non-thermally or hydrometrically controlled environment [27].

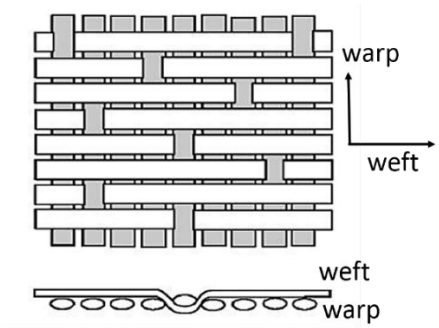


**Figure 1 : Schematic representation of a 8-harness satin composite**


**Figure 2 : Schematic representation of a 2/2 twill composite**

### 2.2 Damage monitoring on composite materials

As well as metallic materials, composite materials can be damaged during their lifetime. However, due to their heterogeneity, composite materials can present several types of damage mechanisms of varied severity [31]–[34] : matrix cracking in the transverse yarn (Figure 3, (b)), fibre-matrix debonding in the warp direction, matrix cracking between warp and weft directions (Figure 3, (c)), warp breakage (Figure 3, (d)) and delamination between layers. To monitor and detect the occurrence and evolution of composite damage mechanisms, different experimental techniques are used, such as acoustic emission or optical microscopy.

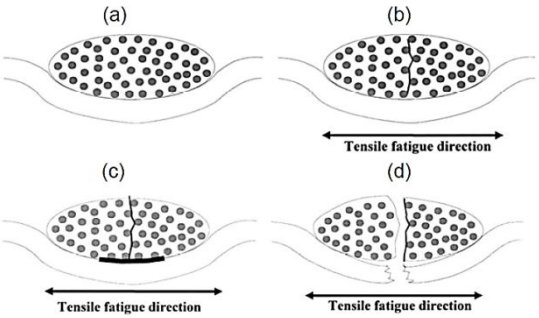


**Figure 3 : Damage evolution scheme in a two dimensional woven composite under tension-tension fatigue loading in the warp direction [34]**

Non-destructive monitoring of the damage can be carried out by optically scanning the edge thanks to a microscope, in order to visually monitor the appearance of cracks. It is then assumed that the damage visible on the edge is representative of the damage caused in within the volume of the sample. In addition, the use of acoustic data can be a complementary technique to confirm the damage evolution. Indeed, damage in a composite material releases elastic energy that propagates as a transient elastic wave, also called acoustic emission. Acoustic emission is detected by piezoelectric sensors. The passive monitoring of the acoustic activity of the material under loading can provide useful data regarding damage evolution [33]-[36].

### 2.3 Thermographic techniques applied to composite materials

The study of progressive damage during quasi-static tensile tests is generally based on the monitoring of mechanical properties, such as the Young modulus or the irreversible strain. Yet, some authors [7], [8], [14]–[16] have also studied the thermal behaviour of neat plastic or thermoset composite materials during a static tensile test. For a long time considered as quasi-constant because of the small temperature variations, it has been noted that thermal behaviour follows a three-step pattern (Figure 4) during the tensile test:

- The first regime (I) corresponds to the elastic mechanical domain of the material: the temperature linearly decreases with the increasing stress.
- The second regime (II) corresponds to the inelastic mechanical behaviour: the temperature decreases non-linearly until a minimum.
- The third regime (III) is characterized by the non-linear increase of the temperature, due to damage apparition, until the sample breaks.

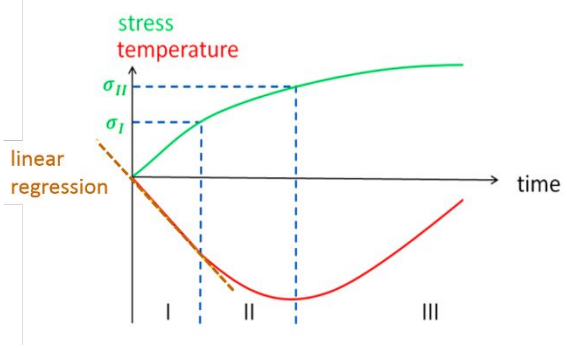


**Figure 4 : Schematic representation of stress and temperature trends during quasi-static tests, and identification of the three temperature regions marked by the threshold stress values $\sigma_I$ and $\sigma_{II}$**

The first domain (I) corresponds to the thermoelastic behaviour of the material; the variation of the heating $\Delta T$ is linked to the stress according to Equation (1) [17], [18] :

$$\Delta T = -T_0 \frac{\alpha}{\rho c_p} \Delta\sigma \quad (1)$$

$T_0$ is the initial average temperature of the sample, $\alpha$ the thermal expansion coefficient in the warp loading direction, $\rho$ the mass density and $c_p$ the specific heat of the composite material. This law is only valid in the elastic domain (part I), until the stress threshold value $\boldsymbol{\sigma_I}$. Thus, the end of linearity of the temperature behaviour marks the end of the thermoelastic domain. This change has been correlated with the beginning of plasticization of neat plastic specimens [8] and with the appearance of micro-damage in thermoset composite materials [14], [15]. Then, the transition between the second and the third thermal regimes is emphasized by a thermal minimum, associated with the stress threshold value $\boldsymbol{\sigma_{II}}$. This transition was correlated to the appearance of macro-damage in [14], [15], which would generate enough heat to balance the cooling of the specimen. It was highlighted that the changes of thermal behaviour could be correlated to the appearance of different types of damage coalescence at the micro and macro scale.

This application of thermography to the monitoring of static tensile tests can be transposed to cyclic loads, hence the self-heating tests. As previously introduced, the self-heating tests are used as an alternative to the conventional, time-consuming fatigue tests to estimate the fatigue limit of the material. In this case, instead of cycling each sample until failure for several given load values, a few number of blocks with a limited number of cycles are applied to the same sample, with increasing load values (Figure 5). During the test, the temperature of the specimen is monitored with thermocouples or an infrared camera. A theoretical evolution of a specimen average heating during one block is given in Figure 6: the surface temperature of the sample increases until a stabilized value. The evolution of the average stabilized temperature of the specimen with the maximal stress value of each block shows two tendencies: for the lowest load values, the stabilized temperature show only a small increase between block 1 and block 3 in Figure 7. After a particular load value, called $\boldsymbol{\sigma_T}$ (for 'threshold'), the stabilized temperature strongly increases (blocks n-1 and n in Figure 7). In the case of metallic materials, self-heating is negligible in the stress range below $\boldsymbol{\sigma_T}$ and is activated by the energy dissipated due to microplastic deformations, initiating microcracks ultimately leading to failure. In the case of composite materials reinforced with organic matrices, the self-heating slowly increases in the stress range below $\sigma_T$, mostly due to the resin viscosity, and is accelerated after $\boldsymbol{\sigma_T}$ by the addition of any kind of damage growth induced by the cyclic loading, such as friction, indicating the initiation of fatigue damage. Therefore, the temperature variation of the sample is mainly due to cracks sliding effect leading to friction (heat sources). Classically the temperature indicator is chosen as the average specimen temperature minus its initial temperature. This approach has been proven efficient for metallic materials [1]–[3], [10], [19] and was successfully applied to some composite materials [4], [13], [20]: the specific stress value $\boldsymbol{\sigma_T}$ between the two thermal tendencies during the self-heating tests is connected to the limit determined on the Wöhler curve. It seems that the self-heating monitoring can indeed enable a reliable monitoring of fatigue damage.

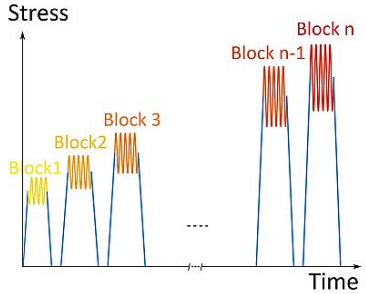


**Figure 5 : Schematic representation of self-heating tests for a fixed R ratio of stress**

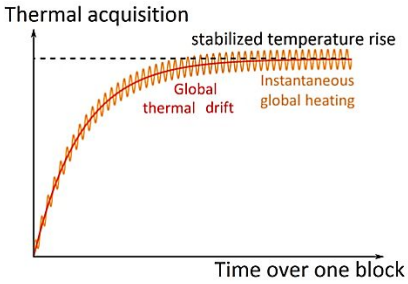


**Figure 6 : Theoretical temperature rise over one block**

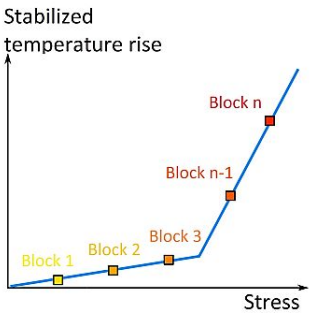


**Figure 7 : Theoretical self-heating curve**

Above all, it has been noted by [16], [21] that for a thermoset composite material, the stress related to the first thermal transition (between I and II) $\boldsymbol{\sigma_I}$ corresponds to the fatigue limit, which can also be determined during self-heating tests through the estimation of the specific stress value $\boldsymbol{\sigma_T}$. This conclusion is worth investigating on other types of composite materials (carbon fibres, thermoset matrix), to verify its generalization. It justifies of our study and is the basis of our approach. Thus, in

[7], [14], [15], thermal monitoring during static and self-heating tests was applied to glass-fibres composite materials. In our study, we will extend this investigation to carbon fibre reinforced materials, and we will further investigate the evolution of the damage by also monitoring the acoustic activity and performing optical scans of the edge, to confirm the connection between heating and damage in both tests.

### 2.4 Mechanical tests

In this study, the quasi-static tensile tests are carried out on a ZWICK electromechanical machine, equipped with mechanical grips and a 150 kN load cell. The applied loading rate is fixed to 2 MPa/s. The samples are rectangular, 250mm long, 25mm wide and 2mm thick. As the thermoplastic material is a balanced woven composite, the mechanical properties are similar in the warp (0°) and weft (90°) direction, as previously verified in [28]: the tests are applied in the warp direction and the results correspond to the fibre behaviour of the materials. In comparison, the unbalanced thermoset composite is tested in the warp direction only. Six samples are tested for both the thermoset and the thermoplastic composite materials.
Their self-heating during the quasi-static test is monitored by a FLIR X6540sc mid-wave infrared camera, used on a [3-5] µm wavelength range, with a 20 mK thermal sensitivity and a space resolution of 640×512 pixels. The acquisition frequency is 50 Hz. The temperature is monitored over the whole surface of the sample and averaged over the rectangular area located between the acoustic sensors (see rectangle in continuous line in Figure 8 b). An equivalent area is also measured on the reference specimen, represented in dashed line in Figure 8 b. Two acoustic sensors are used to record each acoustic emission occurring during the test, with a detection threshold set at 40 dB to filter machine noise [28] (Figure 8 a). The acquisition is done on a frequency band from 20 kHz to 1.2 MHz, and the acquisition system is a PCI-2 system from Mistras Company. An optical microscope with a magnification of 5, not shown on Figure 8, is used to scan one of the free edges of the tested specimen.

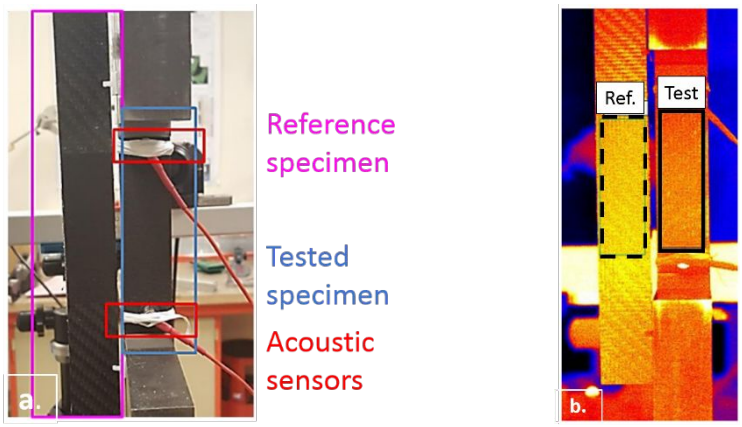


**Figure 8 : Pictures of the experimental set-up of the quasi-static tests. (a) the test specimen equipped with acoustic sensors and the reference specimen (b) representation of the selected zone used for the thermal acquisition.**

The self-heating tests are performed on an INSTRON hydraulic machine with a capacity of 100 kN, equipped with hydraulic jaws. To avoid any resonance effect between the frequencies of the test and of the infrared camera, the frequency of the cyclic load is set to $f = 4.72$ Hz. The load ratio $R$, defined by the ratio between the minimal and the maximal applied stresses, is fixed at $R = 0.5$ for the thermoset composite and $R = 0.1$ for the thermoplastic composite. The tests are built with 12 blocks of 6,000 cycles, with a stress step of respectively 55 MPa and 40 MPa. This set of parameters, determined from existing literature ([13], [20], [28]), enables to cover the whole range of stresses, from near zero to failure (determined by quasi-static tests), with enough steps to monitor any thermal behaviour, and enough cycles per step to ensure a thermal equilibrium. The thermal field is monitored with the same infrared camera as the quasi-static mechanical tests, with the same thermal acquisition area. The acquisition frequency is set to 1 Hz. Two acoustic sensors are used, with the same parameters and acquisition system as the quasi-static tests (Figure 9).

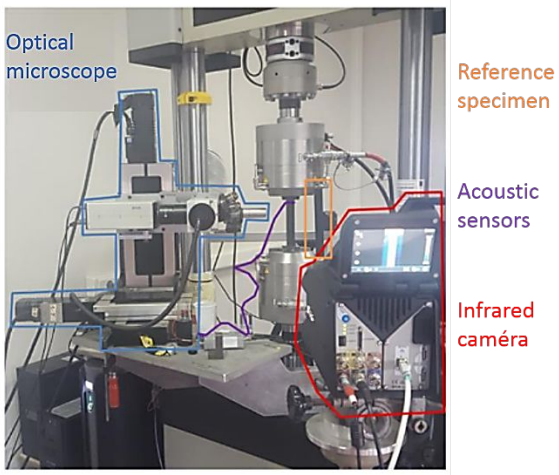


**Figure 9 : Picture of the experimental set-up of the self-heating tests, with the different measuring instruments, the test specimen and the reference specimen.**

## 3. Thermal and damage monitoring during quasi-static and self-heating tests

### 3.1 Quasi-static tests: thermal acquisition

A reference specimen is placed next to the tested specimen under load. Thus, the evolution of the average temperature variation of the tested specimen (average heating θ) is calculated by substracting the average temperature from the reference specimen, to reduce external disturbances:

$$\theta_{\text{specimen}}(t) = T_{specimen}(t) - T_{reference}(t) \quad (2)$$

**Figure 10** shows the result is the case of the thermoplastic composite. The resulting heating is in good agreement with the literature description, with the detection of a linear cooling phase (zone I), a non-linear cooling phase until reaching a thermal minimum (zone II) and a heating phase until the specimen breaks.

To determine the two particular stress values $\boldsymbol{\sigma_I}$ and $\boldsymbol{\sigma_{II}}$ defined in section 2.2, the thermal trend must be extracted from camera noise and ambient disturbances. First, a Gaussian filter is applied, and the filtered signal is subsampled, to decrease the number of data (red, continuous line in Figure 11). Then, the filtered signal is interpolated by the $\ell 1$ trend filtering, a statistical regression method called "segmented regression" : the variables are segmented and a regression analysis is applied to each segment [29], [30]. The thermal curve is interpolated as a succession of linear regressions (black, dashed line in Figure 11) and the number of segments is defined by the $\ell 1$ trend filtering so that the correlation coefficient between the curve and the line is minimized. The accuracy of this minimization can be adjusted according to the $\ell 1$ parameter $\lambda$, which is a regulation parameter used to control a trade-off between the experimental curve segmentation and the residue size. The junctions between two consecutive segments are highlighted by dots. The two particular values that need to be identified are the one associated with the end of the linear domain and the one corresponding to the minimal thermal value.

In order to estimate an interval of confidence, the ambient disturbances, defined by the difference between the thermal signal and the $\ell 1$ trend filtering, is redistributed. To preserve its temporal structure, the kriging method is applied. Thus, the variations of the thermal signal (thermal fluctuation peaks) are assimilated through a Gaussian process, in order to regenerate an ambient disturbance with similar temporal properties. Then, the superposition of this regenerated disturbance on the interpolation of the signal filtered by $\ell 1$-filtering enables several similar thermal signals to be simulated (Figure 12). For each of these simulations, an interpolation by $\ell 1$-filtering is performed to determine the stress levels corresponding to the output of the linearity and the beginning of the

heating. This process is repeated a thousand times, to obtain a Gaussian distribution of the stress estimation. This estimation is then used to calculate a 95% confidence interval (Figure 13). The intervals associated with the particular stress values $\sigma_I$ and $\sigma_{II}$ determined on eight tested samples are given in Table 1.

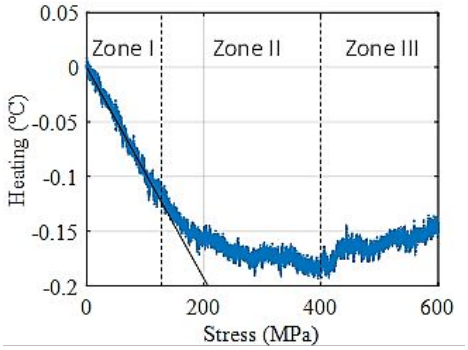


**Figure 10 : Evolution in blue of the spatial average the thermal signal of the sample with the stress during a static test. The three thermal trends described in section 2.1 and the linear part are highlighted with black lines.**

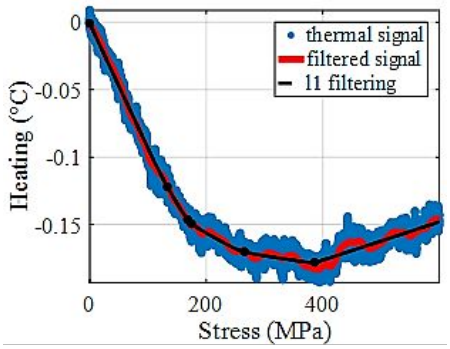


**Figure 11 : A gaussian filtering (in red) is applied on the thermal signal (in blue), and the $\ell 1$ trend filtering (in black) is applied on the filtered signal to interpolate the data as several linear regressions.**

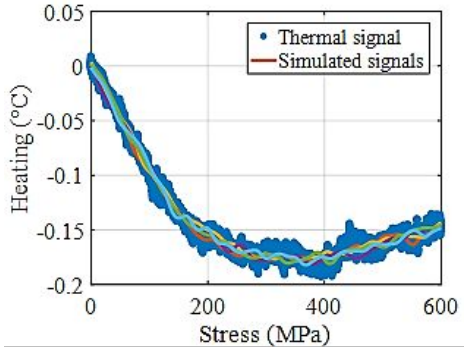


**Figure 12 : Representation of the several simulated signals, considering the measured residuals between the filtered signal and the piecewise linear regression**

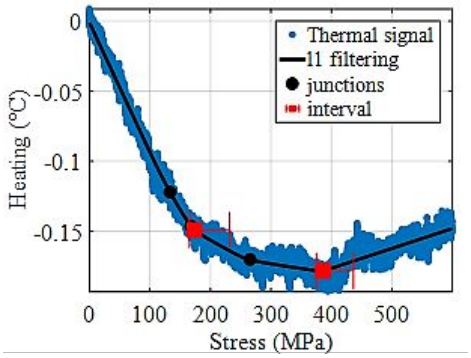


**Figure 13 : Representation in red of the stress values $\sigma_I$ and $\sigma_{II}$ and their confidence interval in the case of thermoplastic material**

**Table 1** : Particular stress values for thermoplastic composite specimens under quasi-static loads

| **Thermoplastic composite Carbon/PA66** | **End of linearity $\sigma_I$** | **Thermal minimum $\sigma_{II}$** |
|---|---|---|
| Sample 1 | [165 - 240] MPa | [465 - 500] MPa |
| Sample 2 | [110 - 160] MPa | [370 - 430] MPa |
| Sample 4 | [90 - 145] MPa | [460 - 520] MPa |
| Sample 5 | [60 - 75] MPa | [425 - 450] MPa |
| Sample 6 | [90 - 120] MPa | [380 - 430] MPa |
| Sample 7 | [50 - 80] MPa | [370 - 420] MPa |
| Average of the extreme values | **[100 – 150] MPa** | **[410-460] MPa** |

The same process is applied to the thermoset composite. The Figure 14 presents the final result, including the intervals of confidence. It seems that the Zone I (linear cooling) and the Zone II (non-linear cooling) are almost coincident, which is more clearly apparent on the focus shown on Figure 15. The intervals associated with the particular stress values determined on six tested samples are given in Table 2 and confirm that the two intervals regularly merge.

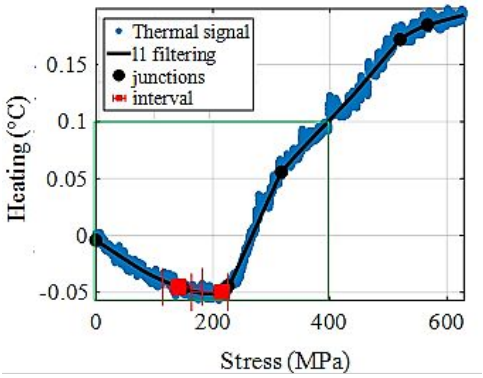


**Figure 14 : Representation in red of the stress values $\sigma_I$ and $\sigma_{II}$ and their confidence interval in the case of thermoset material**

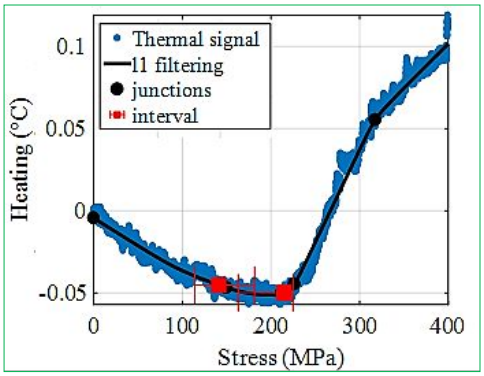


**Figure 15 : Focus of Figure 14 on the [0-400] MPa range**

**Table 2** : Particular stress values for thermoset composite specimens under quasi-static loads

| Thermoset composite Carbon/epoxy | End of linearity $\sigma_I$ | Thermal minimum $\sigma_{II}$ |
|---|---|---|
| Sample 1 | [100 - 170] MPa | [175 - 200] MPa |
| Sample 2 | [30 - 110] MPa | [190 - 225] MPa |
| Sample 3 | [110 - 180] MPa | [160 - 225] MPa |
| Sample 4 | [140 - 185] MPa | [210 - 225] MPa |
| Sample 5 | [90 - 125] MPa | [185 - 215] MPa |
| Sample 6 | [125 - 165] MPa | [205 - 230] MPa |
| Average of the extreme values | **[100 – 160] MPa** | **[190-220] MPa** |

### 3.2 Quasi-static tests: damage

To correlate variations in thermal behaviour to a physical phenomenon, damage monitoring by microscopic observation and acoustic monitoring is performed and presented.

**Optical microscopy**

In order to link the thermal changes to actual damage, several sets of microscopic observations of the polished edge of the specimen are acquired. For both materials, one set of microscopic observations is made before the mechanical test, to determine the initial state of the sample. Then, five sets are made around the threshold stresses associated to the end of the thermal linearity and to the start of the heating, and the last is made shortly before the ultimate failure. The micrographic images provide an overview of the damaged (or undamaged) state of the material, assuming that the edge of the specimen is indeed representative of its inside state. To detect and highlight the appearance of cracks, the pictures from the observation during the initial state are subtracted from the pictures from the observation under loading, to accentuate optical differences. The difference between the two images, highlighted in yellow, is then superimposed on the raw image of the microscope.

The thermoset woven composite material is shown in Figure 16 and Figure 17. The material is shown in its initial state and at the occurrence of the first cracks, highlighted in yellow. These cracks correspond mainly to matrix cracking. Table 3 shows the stress level associated with the first observed cracks for the six tested specimens. It appears that the appearance of the first visible matrix cracks corresponds at $\sigma_{optic} = 235 \pm 40\ MPa$, which is slightly higher than the stress value $\sigma_{II} = [190 - 220]$ MPa associated with the beginning of the heating of the thermoset composite.

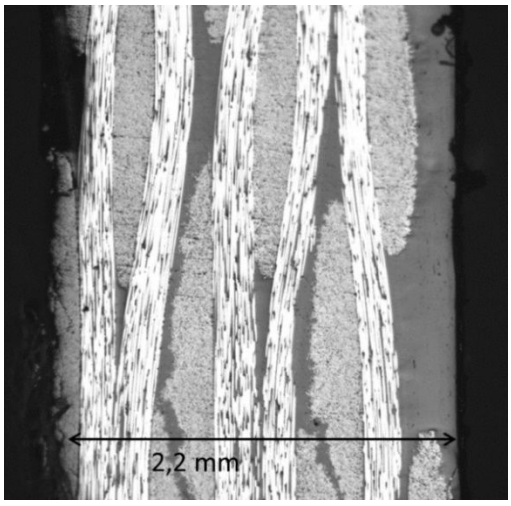


**Figure 16 : Free edge's microscopic observation on the initial state of the thermoset composite Carbon/epoxy**

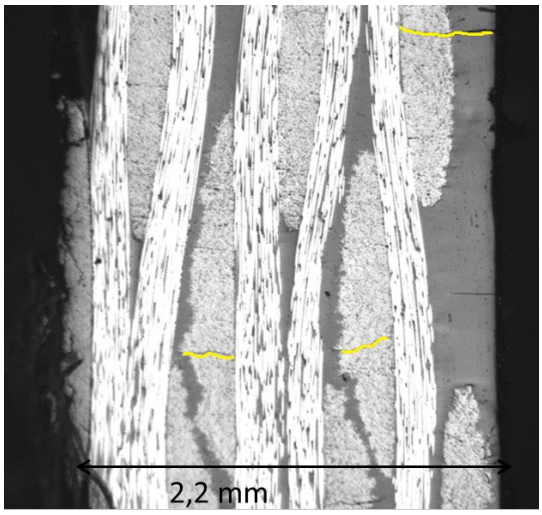


**Figure 17 : Free edge's microscopic observation of the first cracks, highlighted in yellow, of the thermoset composite, at $\sigma = 220\ MPa$**

**Table 3 : Stress level associated with the first cracks for thermoset composite specimens under quasi-static loads**

| | Sample 1 | Sample 2 | Sample 3 | Sample 4 | Sample 5 | Sample 6 |
|---|---|---|---|---|---|---|
| **First cracks** | 220 MPa | 185 MPa | 225 MPa | 240 MPa | 310 MPa | 240 MPa |

In the case of the woven thermoplastic composite, the same process is applied. However, no visible matrix cracks appear during the tests. Figure 18 and Figure 19 show respectively the material in its initial state and just before the failure, at $\sigma = 645\ MPa$, centred around the final fracture zone, to detect the appearance of possible meso cracks (warp scale) that might have initiated the final failure. Based on Figure 19, it seems that no transverse cracks appear. The only visible difference between the two images is most likely noise, associated with the deformation of the material, and/or changes in setting (such as brightness) between the two shots. This is checked for the whole edge of the specimen. It can be concluded that for this thermoplastic material, micrographic observation is not relevant to detect the initiation and/or propagation of damage. This justifies the use of X-ray micro tomography to inspect the inside of the material.

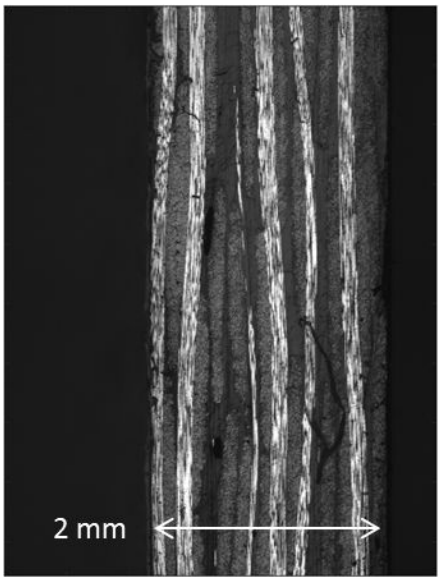


**Figure 18 : Free edge's microscopic observation on the initial state of the thermoplastic composite Carbon/PA66**

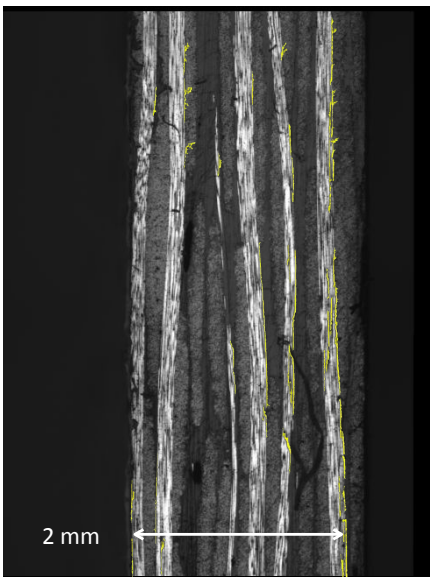


**Figure 19 : Free edge's microscopic observation shortly before failure of the thermoplastic composite, at 645 MPa, highlighting structural changes**

In order to furtherly investigate the possible presence of damage of any kind, a sample previously submitted to a tensile test up to 400 MPa is scanned in an X-ray micro-tomograph, thanks to the participation of the European Synchrotron Radiation Facility ESRF. The aim is to detect if any damage appears at the same stress level that the one associated with the beginning of the heating ($\sigma_{II}$). Figure 20 illustrates the scanned area, in blue colour, of size 2mm*2mm*1.2mm. The pixel size is 0.65 µm and the energy is 20 keV. 2,160 images are acquired. The image presented in Figure 21 is representative of all the observations made on the tomograph. Transverse and longitudinal fibres yarns are identifiable, as well as pure matrix areas. However, no cracks (matrix or intra-yarn) are detected. Even if the observed volume is very small compared to the whole sample (Figure 20), this result matches the one already obtained from optical microscope observations: it is very difficult to detect which type of damage starts at 400 MPa and leads to the heating of the material.

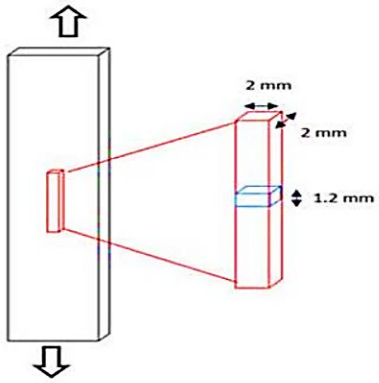


**Figure 20 : Drawing of the tested sample, with the cut-out area (in red) and the area observed with the X-ray micro tomograph (in blue)**

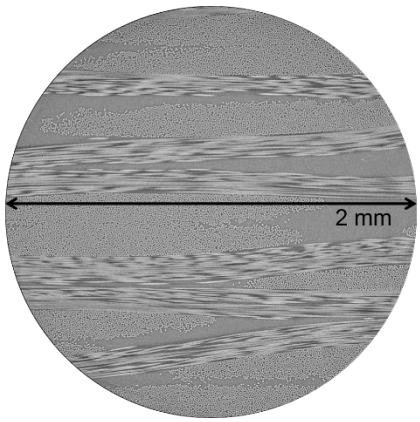


**Figure 21 : View of the thermoplastic sample loaded until 400 MPa and inspected by the X-ray micro tomograph**

## Acoustic emission

The acoustic activity is characterized, among other things, by the amplitude and energy of each emitted hit. The evolution of the cumulative acoustic energy with the applied stress enables to identify a damage threshold, from which it continuously starts increasing, highlighted in purple on Figure 22 and Figure 23. To better represent the accumulation of the energy released during the test, the cumulative energy is plotted as a function of the load level, as shown for the thermoset composite on Figure 22 and for the thermoplastic composite on Figure 23. Coupled with the conclusions from the thermal behaviour monitoring, it appears that in both cases, the continuous occurrence of acoustic energy matches with the stress level from which the material begins to heat up. The combination of the two indicators therefore confirms that it is the damage, detected by acoustic emission, which induces the heating of the material.

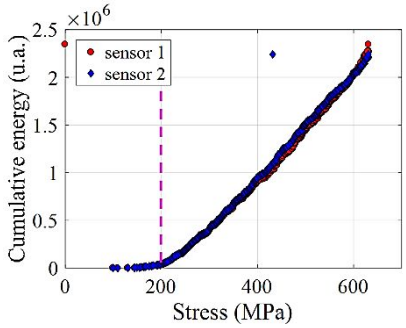


**Figure 22 : Cumulative acoustic energy measured by two acoustic sensors during the quasi-static test on thermoset composite Carbon/epoxy**

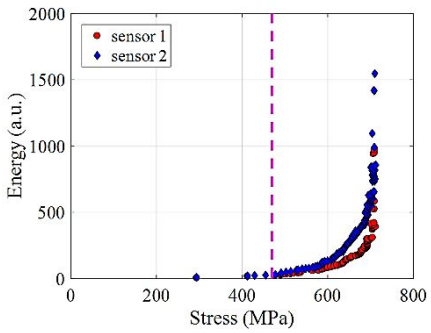


**Figure 23 : Cumulative acoustic energy measured by two acoustic sensors during the quasi-static test on thermoplastic composite Carbon/PA66**

### 3.3 Self-heating tests

**Thermal analysis**

The temperature rise of the sample is determined by subtracting its initial temperature. For each block, the temperature rise solution $\theta$ can be fitted using the Newton's cooling law (heat transfer temperature solution), as follows:

$$\theta(t) = \theta_F\left(1 - \exp\left(-\frac{t}{\tau}\right)\right) \quad (3)$$

with $\theta_F$ the stabilized temperature variation rise and $\tau$ a characteristic time. As shown in Figure 24 for the thermoset composite, the stabilized temperature rise value $\theta_F$ is reached for different stress levels, and tends to increase with the cyclic stress level. The evolution of $\theta_F$ with the maximal stress level of each block leads to the "self-heating curve", displayed in Figure 25. The final result is presented over the [0-400] MPa stress range to better highlight the change of thermal behaviour, which occurs early. The same process is applied for the thermoplastic composite in Figure 26, over the whole [0-600] MPa stress range.

To estimate the change of thermal behaviour, a fitting of the self-heating curve is performed in both cases with two linear regressions, beginning with few experimental data, and increasing the number of data until the whole curve is considered. This methodology has been validated as one of the most robust to correctly determine the change of thermal behaviour, and consequently to link it to the fatigue limit, on a large set of composite materials [35]. The particular stress associated with the thermal change is given by the intersection between the two linear regressions which have the best correlative coefficient. Then, the data is randomly redistributed several times (N = 1000) to simulate several tests with a bootstrap process, and the new intersection is calculated for each random redistribution. Table 4 gives the range associated with the thermal change for the tested samples.

In particular, the results found for the thermoplastic material can be successfully compared to results found in literature. Self-heating tests were performed on this woven carbon/thermoplastic composite material by [13]. The authors used an MTS 880-100kN machine, equipped with hydraulic grips, to test rectangular specimens of nominal dimensions 250x30 mm, with a $[0]_8$ warp stacking sequence. Figure 27 shows the resulting self-heating curve: two thermal trends can be identified, and the change of thermal behaviour occurs around 390 MPa, which corroborates the value found in the present article. Moreover, in [13], it was verified that the change of thermal behaviour determined by the self-heating tests was indeed related to the fatigue limit defined by the fatigue tests, with $\sigma_D = 400\ MPa$, confirming for this composite material this hypothesis made at the beginning of the article on the link between fatigue and self-heating.

**Table 4 : Change of thermal behaviour for 0° specimens under cyclic loads**

| | Change of thermal behaviour Thermoplastic material Carbon/PA66 | Change of thermal behaviour Thermoset material Carbon/epoxy |
|---|---|---|
| **Sample 1** | [315 - 435] MPa | [160-220] MPa |
| **Sample 2** | [315 - 405] MPa | |

It is very promising that these estimation ranges are close to the estimation ranges determined during the quasi-static tests, in particular with the values associated to the beginning of heating. It appears that in both tests, a change of thermal behaviour occurs at the same load level. The goal is now to verify that this thermal change is associated with the emergence of damage during the self-heating tests, as it was during the quasi-static tests, with the use of optical observation and acoustic monitoring.

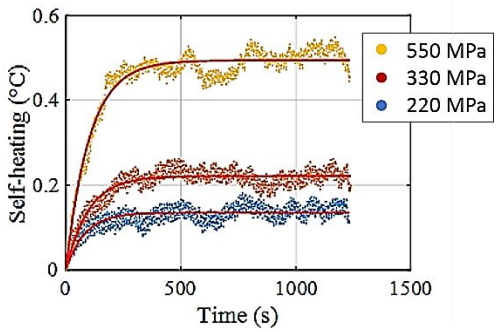


**Figure 24 : Variation of temperature rise from one stress level to another for the thermoset composite Carbon/epoxy**

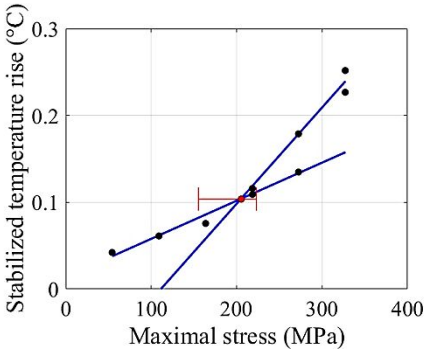


**Figure 25 : Self-heating curve obtained for the thermoset composite Carbon/epoxy**

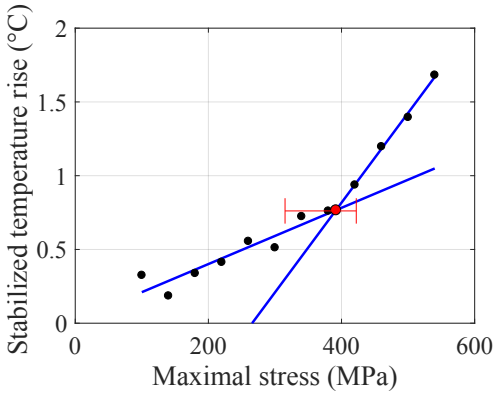


**Figure 26 : Self-heating curve obtained for the studied thermoplastic composite Carbon/PA66**

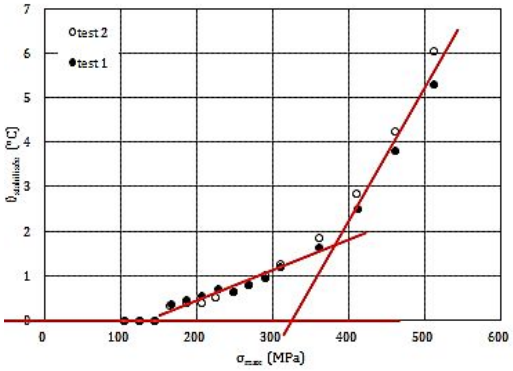


**Figure 27 : Self-heating curve obtained by [13] on the same woven Carbon/PA66 composite**

## Optical microscopy

The progressive appearance of cracks is monitored under load. Before each cyclic step, the specimen is kept in position at the maximum stress applied during the following step to keep the cracks opened. The microscope then scans the edge of the specimen at a magnification of x5.

In the case of the thermoplastic composite, as no damage had occurred during the quasi-static tests, it is again the last level that is observed as a priority. However, no clear cracks appear on the edge of the sample during the last monotonous loading phase. No cracks therefore appear a posteriori during monotonous loading phases or during cyclic loading phases, indicating a future failure zone.

On the other hand, in the case of thermosetting composite, the material shows progressive damage as the maximal load gradually increases. Thus, matrix cracking occurs from 200 MPa. Further damage then occurs, from 300 MPa, such as debonding and delamination. The Figure 28 shows the evolution of matrix cracking in the same area of the specimen, for three loading levels. It is thus verified that the change in thermal behaviour observed on the self-heating curves is associated with the appearance of the first damage, i.e. the first matrix cracks.

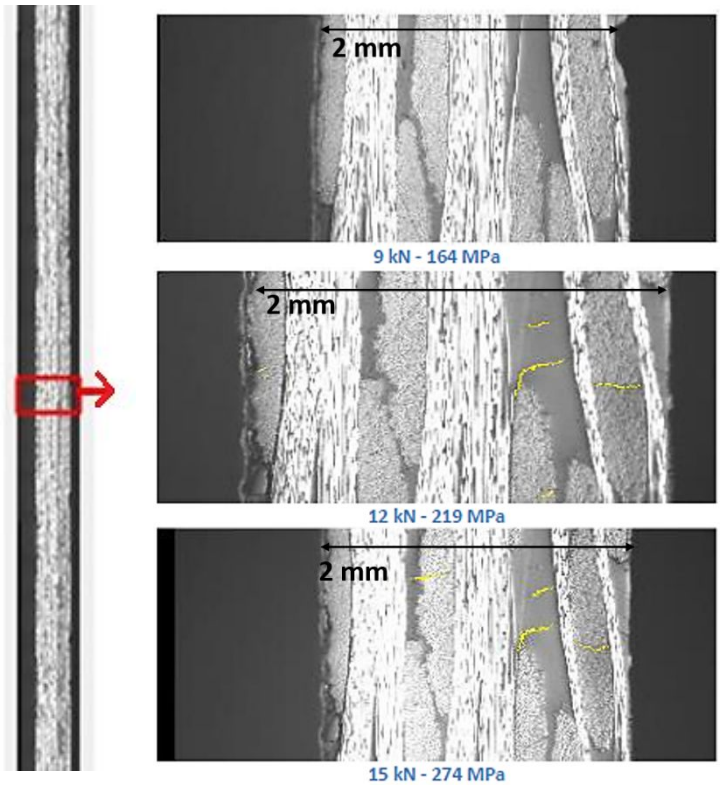


**Figure 28 : Evolution of the same area of the sample of carbon/epoxy composite during three cyclic steps**

## Acoustic emission

Since the loading sequence is a succession of blocks of mechanical cycles, it is no longer possible to present the cumulative energy according to the applied stress. Figure 29 and Figure 30 therefore show in two different axes the applied stress, in black, and the cumulative energy recorded by the two sensors, in blue and red, in the case of the thermoset and thermoplastic composite. The damage threshold, which is assumed to have been reached when the acoustic emission becomes continuous, is shown in magenta dots on Figure 29 at a value of $\sigma_{max} = 170\ MPa$ and on Figure 30 at a value of $\sigma_{max} = 410\ MPa$. These values are close to the stress level associated with the change of thermal behaviour and the appearance of micro-cracks in the case of the thermoset composite. Thus, the acceleration of the heating observed in Figure 25 and Figure 26 corresponds to the same load levels from which acoustic emission significantly appears.

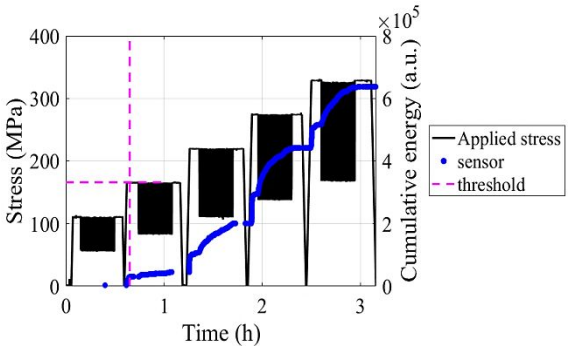


**Figure 29 : Cumulative acoustic energy of each sensor during a self-heating test, and acoustic damage threshold, for the thermoset composite Carbon/epoxy. The self-heating tests are carried out at R=0.1, with a return to zero load between each block.**

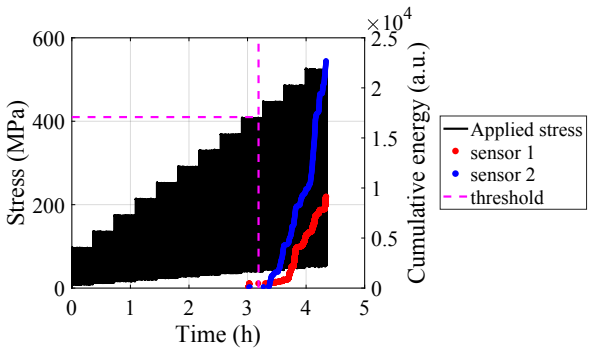


**Figure 30 : Cumulative acoustic energy of each sensor during a self-heating test, and acoustic damage threshold, for the thermoplastic composite Carbon/PA66. The self-heating tests are carried out at R=0.5, without a return to zero lead between each block.**

## 4. Discussion

Heat transfer study is the main idea of the proposed paper to obtain rapidly the fatigue limit in the warp direction of woven materials. Compared to the previous work [28], this new study has made it possible to validate a simple improvement of the experimental protocol by adding the thermal monitoring of a reference specimen. This process enables to extract the specific temperature variations of the specimen by removing any contributions from environment with the help of a reference specimen. Thus, in the case of quasi-static tests, the three thermal trends described in the literature are checked, and the self-heating curves show a low noise level, even at low stresses, which enables to successfully apply statistical processing tools.

Therefore, the thermal monitoring of quasi-static tests shows that the thermal behaviour of the thermoplastic and thermoset composites under monotonic loading corresponds to the thermal behaviour described in several works dedicated to glass-fibres thermoset composite materials ([14], [15], [21]). It is then confirmed that such thermal analysis can be extended to other types of composite materials. Moreover, the use of statistical tools has made it possible to properly determine the threshold stresses associated with the end of the thermoelastic linearity and the start of the heating and to assess error bars which are essential given the small temperature variations that are monitored. In the case of thermoset composite materials, the zone II is almost non-existent, and only the thermal minimum seems to be a relevant thermal indicator. In fact, the end of linearity is more difficult to visualize and determine, and the associated charge level is influenced by the configuration of the filter.

Based on microscopic observations, variations in thermal change are related by [14], [15], [21] to the occurrence of damage, such as matrix cracking, and the stress assimilated to the first thermal change $\boldsymbol{\sigma_I}$ related to the fatigue limit: under this stress, the material does not present micro damage appearance. However, for the present thermoset and thermoplastic composite materials, observation of the edge under the microscope showed that in the case of thermoset composite, the appearance of micro-cracks coincided more with the heating of the material, associated with the stress level $\boldsymbol{\sigma_{II}}$. This link is corroborated with the emergence of acoustic emission. Similarly, even if no visible damage appears at the micro-scale in the case of the thermoplastic composite, the emergence of continuous acoustic emission seems to concur with the second thermal change, associated with the start of the heating of the specimen.

The same process applied to self-heating tests leads to similar conclusions. The self-heating of the composite materials reaches a stabilized heating value at each step, numerically determined with statistical tools along with the confidence interval. In the case of thermoplastic composites, the evolution of the self-heating with the stress level is found in good agreement with [13], which validates both our experimental protocol and our data analysis procedure. Moreover, the optical scanning of the tested specimen edges confirms that micro damage occurs at the same load level than the one associated with thermal changes and the start of continuous acoustic emission. It is therefore assumed that for both mechanical tests, the initial heating of the materials is mainly related to the viscosity of the matrix, while the acceleration of the heating indicates the emergence of the damage through crack friction.

Therefore, not only damage is the same under monotonic and cyclic loadings, but also the coupling between thermal and acoustic monitoring leads to the same conclusions: the beginning of matrix cracking both induces acoustic emission and a higher heating. It is very interesting to note that these phenomena are observed for both types of loading, and, most importantly, occur for the same load levels. Consequently, the thermal monitoring of a fast-monotonic tensile test can provide comparable information as a self-heating test, in the case of thermosetting or thermoplastic matrix composites, loaded in the direction of the fibres. Moreover, it has been assumed, and verified by [13] for the thermoplastic composite, that the acceleration of the heating during the self-heating tests occurs when the fatigue limit is reached. It can then be concluded from this article that this alleged fatigue limit can even be estimated from monotonic tensile tests.

These results, although promising, do not claim to definitely validate the use of quasi-static or self-heating tests to estimate the fatigue limit of composite materials. The very existence of a fatigue limit remains mostly theoretical and is commonly replaced by an endurance limit at $10^x$ cycles (with $x$ equal to 7 at least). The stress thresholds identified by the thermal monitoring of much faster static or dynamic tests appear to be similar to these endurance limits, hence the relevance of the present study. Moreover, our work made it possible to undoubtedly link the evolution of the heating of the tested composites to actual damage observed with optical microscopy (matrix cracking, mostly) and to acoustic events.

## 5. Conclusion

Infrared thermography is widely used for the non-destructive inspection of composite materials as well as for their monitoring under static or dynamic mechanical loading. The present study aimed at assessing and comparing the thermal behaviour of two carbon-fibre woven composites, respectively with a thermoset and a thermoplastic matrix, during quasi-static tests and self-heating tests. Moreover, during both tests, thermal data was confronted to acoustic data and *post-mortem* optical images in order to improve the understanding of the detected heating changes and to link them to physical phenomena.

Several conclusions can be deduced from this study. For both static and cyclic loadings, the coupling of heating monitoring and acoustic emission enables to validate a damage scenario, associated with a beginning or an acceleration of the temperature rise and the start of acoustic events: matrix cracking and fibres failure. For the thermoset composite, the microscopic observations show a progressive evolution of the damage, starting with matrix cracking, followed by debonding. For the thermoplastic composite, since no damage is visible in the microscopic observations, it can be assumed that the damage of the studied composite material is localized in intra yarns. Most importantly, this study highlights the fact that the recorded thermal and acoustic data occur at the same load level in both static and cyclic tests, as soon as the first matrix cracks appear. Based on previous studies, in particular the one detailed in [13] which sets the equivalence between the load threshold associated with the self-heating acceleration and the fatigue limit for this thermoplastic material, it can be concluded that this limit could actually be estimated by standard, tensile tests. This is a significant breakthrough as it would considerably reduce the duration and the cost of the experimental campaigns currently carried out for the fatigue dimensioning of composite structures.

**Acknowledgements**
The authors wish to thank the Cetim and the ESRF institutes for their support to perform the X-ray micro-tomography.

**References**

[1] M. P. Luong, 'Infrared thermographic scanning of fatigue in metals', *Nuclear Engineering and Design*, vol. 158, no. 2–3, pp. 363–376, 1995.
[2] G. La Rosa and A. Risitano, 'Thermographic methodology for rapid determination of the fatigue limit of materials and mechanical components', *International journal of fatigue*, vol. 22, no. 1, pp. 65–73, 2000.
[3] C. Doudard, S. Calloch, F. Hild, and S. Roux, 'Identification of heat source fields from infrared thermography: Determination of "self-heating" in a dual-phase steel by using a dog bone sample', *Mechanics of Materials*, vol. 42, no. 1, pp. 55–62, Jan. 2010.
[4] L. Jégou, Y. Marco, V. Le Saux, and S. Calloch, 'Fast prediction of the Wöhler curve from heat build-up measurements on Short Fibre Reinforced Plastic', *International Journal of Fatigue*, vol. 47, pp. 259–267, Feb. 2013.
[5] L. Gornet, O. Westphal, C. Burtin, J. L. Bailleul, P. Rozycki, and L. Stainier, 'Rapid Determination of the High Cycle Fatigue Limit Curve of Carbon Fibre Epoxy Matrix Composite Laminates by Thermography Methodology: Tests and Finite Element Simulations', *Procedia Engineering*, vol. 66, pp. 697–704, 2013.

[6] A. Katunin and D. Wachla, 'Determination of fatigue limit of polymeric composites in fully reversed bending loading mode using self-heating effect', *Journal of Composite Materials*, vol. 53, no. 1, pp. 83–91, Jan. 2019
[7] C. Colombo, F. Libonati, F.Pezzani, A. Salerno, and L. Vergani, 'Fatigue behaviour of a GFRP laminate by thermographic measurements', *Procedia Engineering*, vol. 10, pp. 3518–3527, 2011
[8] C. Clienti, G. Fargione, G. La Rosa, A. Risitano, and G. Risitano, 'A first approach to the analysis of fatigue parameters by thermal variations in static tests on plastics', *Engineering Fracture Mechanics*, vol. 77, no. 11, pp. 2158–2167, Jul. 2010.
[9] N. E. Dowling, *Mechanical Behaviour of Material : Engineering methods for deformation, fracture, and fatigue*, International Edition. Pearson, 2013.
[10] R. Munier, C. Doudard, S. Calloch, and B. Weber, 'Identification of the micro-plasticity mechanisms at the origin of self-heating under cyclic loading with low stress amplitude', *International Journal of Fatigue*, vol. 103, pp. 122–135, Oct. 2017
[11] M. Poncelet, C. Doudard, S. Calloch, F. Hild, B. Weber, and A. Galtier, 'Prediction of self-heating measurements under proportional and non-proportional multiaxial cyclic loadings', *Comptes Rendus Mécanique*, vol. 335, no. 2, pp. 81–86, Feb. 2007
[12] L. Jegou, Y. Marco, V. Le Saux, and S. Calloch, 'Fast prediction of the Wöhler curve from heat build-up measurements on Short Fibre Reinforced Plastic', *International Journal of Fatigue*, vol. 47, pp. 259–267, Feb. 2013
[13] C. Peyrac, T. Jollivet, N. Leray, F. Lefebvre, O. Westphal, and L. Gornet, 'Self-heating Method for Fatigue Limit Determination on Thermoplastic Composites', *Procedia Engineering*, vol. 133, pp. 129–135, 2015
[14] L. Vergani, C. Colombo, and F. Libonati, 'A review of thermographic techniques for damage investigation in composites', *Frattura ed Integrità Strutturale*, 2014.
[15] F. Libonati and L. Vergani, 'Damage assessment of composite materials by means of thermographic analyses', *Composites Part B: Engineering*, vol. 50, pp. 82–90, Jul. 2013
[16] L. Gornet *et al.*, 'Propriétés mécaniques en fatigue à grands nombres de cycles des composites carbone époxy', *Revue des composites et des matériaux avancés*, vol. 25, no. 2, pp. 181–200, 2015
[17] W.-T. Kim, M.-Y. Choi, Y.-H. Huh, and S.-J. Eom, 'Measurement of thermal stress and prediction of fatigue for STS using Lock-in thermography', *Proc. 12th A-PCNDT*, 2006.
[18] A. Salerno, A. Costa, and G. Fantoni, 'Calibration of the thermoelastic constants for quantitative thermoelastic stress analysis on composites', *Review of Scientific Instruments*, vol. 80, no. 3, p. 034904, Mar. 2009
[19] M. Poncelet, C. Doudard, S. Calloch, F. Hild, B. Weber, and A. Galtier, 'Prediction of self-heating measurements under proportional and non-proportional multiaxial cyclic loadings', *Comptes Rendus Mécanique*, vol. 335, no. 2, pp. 81–86, Feb. 2007
[20] L. Gornet, O. Westphal, A. Krasnobrizha, P. Rozycki, C. Peyrac, and F. Lefèbvre, 'Rapid determination of the high cycle fatigue limit of a woven carbon fibe thermoplastic matric', *JNC 19*, 2015.
[21] C. Colombo, F. Libonati, F. Pezzani, A. Salerno, and L. Vergani, 'Fatigue behaviour of a GFRP laminate by thermographic measurements', *Procedia Engineering*, p. 11, 2011.
[22] A. Doitrand, C. Fagiano, F. Hild, V. Chiaruttini, A. Mavel, and M. Hirsekorn, 'Mesoscale analysis of damage growth in woven composites', *Composites Part A: Applied Science and Manufacturing*, vol. 96, pp. 77–88, May 2017
[23] A. Malpot, F. Touchard, and S. Bergamo, 'Effect of relative humidity on mechanical properties of a woven thermoplastic composite for automotive application', *Polymer testing*, vol. 48, pp. 160–168, 2015.
[24] M. Broudin *et al.*, 'Water diffusivity in PA66: Experimental characterization and modeling based on free volume theory', *European Polymer Journal*, vol. 67, pp. 326–334, Jun. 2015
[25] A. Benaarbia, A. Chrysochoos, and G. Robert, 'Influence of relative humidity and loading frequency on the PA6.6 cyclic thermomechanical behaviour: Part I. mechanical and thermal aspects', *Polymer Testing*, vol. 40, pp. 290–298, Dec. 2014.
[26] L. Greenspan, 'Humidity Fixed Points of Binary Saturated Aqueous Solutions', *A. Physics and Chemistry*, vol. 81 A, 1977.
[27] A. Malpot, F. Touchard, and S. Bergamo, 'Influence of moisture on the fatigue behaviour of a woven thermoplastic composite used for automotive application', *Materials & Design*, vol. 98, pp. 12–19, 2016.
[28] L. Muller *et al.*, 'Experimental monitoring of the self-heating properties of thermoplastic composite materials', *Procedia Engineering*, vol. 213, pp. 183–191, 2018
[29] S.-J. Kim, K. Koh, S. Boyd, and D. Gorinevsky, 'l1 Trend Filtering', *SIAM Review*, vol. 51, no. 2, pp. 339–360, May 2009
[30] A. Moghtaderi, P. Borgnat, and P. Flandrin, 'Trend filtering : Empirical Mode Decompositions versus l1 and Hodrick-Prescott', *Advances in Adaptive Data Analysis*, vol. 03, no. 01n02, pp. 41–61, Apr. 2011

[31] R. D. Adams and P. Cawley, 'A review of defect types and nondestructive testing techniques for composites and bonded joints', p. 15, 1988.
[32] J.-M. Berthelot, 'Transverse cracking and delamination in cross-ply glass-fibre and carbon-fibre reinforced plastic laminates: Static and fatigue loading', *Applied Mechanics Reviews*, vol. 56, no. 1, p. 111, 2003.
[33] R. Talreja, 'Assessment of the fundamentals of failure theories for composite materials', *Composites Science and Technology*, vol. 105, pp. 190–201, Dec. 2014
[34] S. D. Pandita, G. Huysmans, M. Wevers, and I. Verpoest, 'Tensile fatigue behaviour of glass plain-weave fabric composites in on- and off-axis directions', *Composites Part A: Applied Science and Manufacturing*, vol. 32, no. 10, pp. 1533–1539, Oct. 2001
[35] J. Huang, M.-L. Pastor, C. Garnier, and X. Gong, 'Rapid evaluation of fatigue limit on thermographic data analysis', *International Journal of Fatigue*, vol. 104, pp. 293–301, 2017.